Available online at www.sciencedirect.com
ScienceDirect
ELSEVIER
Journal of the European Ceramic Society 27 (2007) 2061–2067
www.elsevier.com/locate/jeurceramsoc

Synthesis of nanosized zirconium carbide by a sol–gel route

Mickael Dollé[a], Dominique Gosset[a,*], Christine Bogicevic[b],
Fabienne Karolak[b], D. Simeone[a], G. Baldinozzi[b]

[a] *CEA Saclay, Laboratoire d'Analyse Microstructurale des Matériaux, DMN/SRMA, 91191 Gif sur Yvette, France*
[b] *Laboratoire Structures, Propriétés et Modélisation des Solides, CNRS UMR 8580, Ecole Centrale Paris, Grande voie des vignes, 92295 Chatenay Malabry cedex, France*

Received 4 May 2006; received in revised form 21 June 2006; accepted 23 June 2006
Available online 8 September 2006

Abstract

Nanosized zirconium carbide was synthesized by a new simple sol–gel method using zirconium *n*-propoxide, acetic acid as chemical modifier, and saccharose as carbon source. When heat-treated at 900 °C under flowing argon, gels transformed into intimately mixed amorphous carbon and nanosized tetragonal ZrO_2. Further heat treatments above 1200 °C led to the formation of zirconium carbide with some dissolved oxygen in the lattice. Oxygen content could be reduced by increasing the heat treatment temperature from 1400 to 1600 °C, which unfortunately also induced a mean crystallites size increase from 90 to 150 nm. Short heat treatments above 1600 °C were carried out to further purify the samples and to limit the particles growth. A compromise between purity and average crystallite's size could then be found. Powders were assessed using X-ray diffraction, thermal analysis and scanning electron microscopy.

Keywords: Sol–gel processes; Grain-size; Carbides; Nuclear applications

1. Introduction

The development of a new generation of nuclear reactors (Gen-IV project),[1,2] with improved thermodynamic yield and a drastic reduction of waste production, requires new materials able to withstand very high temperatures (1000–1200 °C in normal conditions, up to 1500 °C in incidental ones) without performances loss. Metal alloys can no longer meet these specifications and highly refractory compounds such as graphite or silicon carbide, monolithic or composites must be considered. Moreover, in the case of fast-neutron reactors required for efficient nuclear waste burning, low-Z materials are not suitable due to their high neutron slowing-down efficiency. Other compounds are more appropriate, in particular, transition metal carbides like ZrC and TiC. These materials are highly refractory,[3] have a good thermal conductivity,[4] a low neutron absorption and a small absorption cross sections, a weak damage sensitivity under irradiation.[5,6] Unfortunately, they are characterized by brittle mechanical behaviour.[7]

Over last years, nanosized grain materials have shown increasing interests due to new properties, which arise for example from the absence of extended defects in these particles.[8] In fact, unusual mechanical properties are expected in such materials, where the usual characteristic distance between two defects (e.g. dislocations) is larger than the grain-size; moreover the fraction of atoms at the grain boundaries is no longer negligible when it is compared to the bulk material. The increased effect of grain boundaries can be responsible for the onset of new properties such as superplasticity[9] or toughening even in the case of brittle (matrix) materials. In ceramics, few results were published, showing a remarkable improvement of the mechanical properties in some systems such as YSZ.[10] In the case of transition metals nitrides and carbides, diphasic systems such as TiC–TiN or SiC–Si_3N_4[11] were also studied, but no accurate data exists concerning the mechanical properties of pure nanosized carbide ceramics.

Therefore, we have focused our attention on the elaboration of nanosized ZrC powders in order to test the potentialities of this material against two different directions; improving of their mechanical properties (toughness and yield) and analysing their behaviour under irradiation (defect clustering and swelling). The crucial point is to study these properties in compounds as pure

---

[*] Corresponding author. Tel.: +33 169 085857; fax: +33 169 087130.
E-mail address: dominique.gosset@cea.fr (D. Gosset).

0955-2219/$ – see front matter © 2006 Elsevier Ltd. All rights reserved.
doi:10.1016/j.jeurceramsoc.2006.06.005

as possible, easily and cheaply prepared in large quantities by a simple process scalable at an industrial level. The current commercial method for producing MC carbide powders consists of direct reaction of M metal with carbon or by carbothermal reduction of the M_xO_y oxide. Recent studies suggest carbides can be obtained by carbothermal reduction of a precursor, generally prepared by sol–gel process.[12,13] The advantage of using a gel instead of a physical mixture of the solid compounds is the high intimacy at a molecular or colloidal scale. The shorter diffusion distance helps to decrease the heat treatment (dwell temperature and duration) resulting in smaller particles sizes.[14] Sol–gel processing involves the use of molecular precursors, mainly alkoxides, as starting materials. However, most alkoxides are known to react spontaneously with water to form a viscous precipitate; therefore, they require to be chemically modified in order to control their hydrolysis and condensation.[15] In the case of ZrC, gel precursors were obtained by hydrolysis of zirconium alkoxides chemically modified by acetylacetone.[14,16] However, both papers pointed out the formation of oxycarbides with relatively high oxygen content, highly detrimental for mechanical application. Another way to control the alkoxides hydrolysis is to use acetic acid as chemical modifier.[15,17] Such sol–gel process was already investigated for TiC synthesis using saccharose as carbon source[13] and TiC formation with low oxygen content was reported. Surprisingly, this process was not investigated yet for ZrC synthesis. This paper deals with the discussion of a new sol–gel route, using acetic acid as modifier, to obtain nanosized ZrC.

The powders obtained after heat treatments at different temperatures under argon flow were characterized by X-ray diffraction (XRD) to determine the cell parameters and the crystallites size evolution, and by scanning electron microscopy (SEM) to describe the powders morphology. Thermal analyses were carried out to follow the oxidation behaviour under air of the successive powders (precursors and carbides). The heat treatment effect on the lattice parameter and the crystallites size was then determined and these results were used to assess the phase purity (free carbon and oxygen contents).

2. Experimental procedure

The starting chemicals were zirconium *n*-propoxide $Zr(OPr)_4$ (70% in propanol, Fluka), acetic acid AcOH (100% RP Normapur, VWR) and saccharose (Rectapur, VWR).

The preparation of the precursor for ZrC consists of progressively dissolving saccharose (S) in acetic acid kept at 80 °C. Then, the solution is cooled down to room temperature and zirconium *n*-propoxide (ZP) is added under continuous stirring. Immediately, a brown solution is obtained and gelling begins. After 3 h, the solution viscosity has increased; heating at 80 °C evaporates the residual acetic acid and the generated acetates. The so-formed gel is then dried to powder at 120 °C. This dried powder was ground in a vibrating grinder for 1 h before being placed in a graphite boat to undergo the carbothermal reduction. The reduction was performed between 1400 and 1800 °C under flowing argon atmosphere for 3 h in a Pyrox furnace equipped with graphite resistor and matrix.

XRD patterns were recorded using an Inel diffractometer equipped with a curved position sensitive detector (CPSD) using monochromatic Cu $K\alpha_1$ radiation ($\lambda = 1.54052$ Å). Rietveld refinements were carried out at room temperature using the XND program[18] to determine the structural information, the crystallites size and the microstrain.

Sample weight losses during oxidative combustion were monitored by simultaneous thermal gravimetric analysis and differential scanning calorimetry TGA/DSC (Calvet TG-DSC111 using the B111 symmetrical microbalance–Setaram, France).

The morphological information of the different samples were determined by scanning electron microscopy using a FEI Quanta 200.

3. Results and discussion

3.1. Chemistry of gel formation

In sol–gel processing, inorganic metal salts or metal organic compounds such as metal alkoxides are combined with a mixture of solvents (mostly water) to form a sol or a gel. The metal precursors are partially, or completely, hydrolysed and condensed after mixing. The amount of water in the mixture must be precisely controlled to form a sol, with a proper viscosity, or a gel. However, metal alkoxides are well known to react spontaneously with water and to form precipitates resulting from successive hydrolysis and condensation reactions. In order to obtain a sol or a gel, zirconium *n*-propoxide must then be chemically modified by a complexing agent to decrease the alkoxide reactivity with water. Several works have shown that metal alkoxides can be modified by acetic acid, which acts as bridging and chelating ligands[19,20] with the formation of acetates by substitution of (OPr) by (OAc) groups.[17]

Basically, the general reactions occurring during the precursor preparation are metal chelate formation, transesterification and hydrolysis—condensation. The first reaction taking place when zirconium *n*-propoxide is added into acetic acid is the formation of zirconium propoxide diacetate $Zr(OAc)_2(OPr)_2$.[17] This carboxylatoalkoxide can then react following different competitive reactions. The first one is the transesterification of alkoxy groups in $Zr(OAc)_2(OPr)_2$, which react with the saccharose OH groups according to Eq. (1):

$$\begin{aligned}&\mathrm{PrO{-}Zr(OAc)_2(OPr) + HO{-}X{-}(OH)_7}\\&\quad\rightarrow \mathrm{PrO{-}Zr(OAc)_2{-}O{-}X{-}(OH)_7 + PrOH}\end{aligned}\qquad(1)$$

where X is a simplified notation for $C_{12}H_{14}O_3$.

The second reaction occurs between the unreacted acetic acid and the propanol (solvent and product of reaction (1)) to form water and propyl acetate (Eq. (2)):

$$\mathrm{AcOH + PrOH \rightleftarrows PrOAc + H_2O}\qquad(2)$$

The so generated water and the zirconium propoxide diacetate react spontaneously in a substitution reaction (Eq. (3)), in which hydroxy groups replace propoxy groups to generate propanol:

$$\mathrm{Zr(OAc)_2(OPr)_2 + H_2O \rightarrow Zr(OAc)_2(OPr)OH + PrOH \xrightarrow{H_2O} Zr(OAc)_2(OH)_2 + PrOH} \quad (3)$$

As the water formed in reaction (2) is consumed for the hydrolysis, the Eq. (2) equilibrium is then driven to the right as long as enough acetic acid will be present in the solution. This is the reason why a high acetic acid/Zr molar ratio has been chosen to ensure a complete reaction.

Another reaction, which might occur, is the generation of oxo ligands by non-hydrolytic condensation and elimination of an ester (Eq. (4)):

$$\mathrm{2Zr(OAc)_2(OPr)_2 \rightarrow (PrO)Zr–O–Zr(OAc) + PrOAc} \quad (4)$$

Once the different molecules with hydroxy groups are formed ($\mathrm{Zr(OPr)_2(OH)_2}$, $\mathrm{Zr(OAc)_2(OPr)–O–X–(OH)_7}$), further condensation reactions occur leading to an increase of the solution viscosity associated to the formation of Zr–O–Zr and Zr–O–X–O–Zr bridges. After 3 h under continuous stirring, a polymeric precursor is obtained and is placed under heating at 80 °C to evaporate the residual acetic acid and the different generated acetates. The gelled precursor is then collected and completely dried in an oven at 120 °C.

In order to produce stoichiometric ZrC by carbothermal reduction, it was necessary to adjust the carbon/Zr molar ratio to 3 in agreement with Eq. (5):

$$\mathrm{ZrO_2(s) + 3C(s) \rightarrow ZrC(s) + 2CO(g)} \quad (5)$$

Different precursors were then prepared by modifying the ZP/S ratio in the gel composition. These precursors were then pyrolysed to 900 °C in a graphite furnace (Pyrox) at 20 °C/min rate under argon flow with an isotherm of 10 min. This heat treatment was necessary and sufficient to decompose the precursors and to obtain mixed $\mathrm{ZrO_2}$ and amorphous carbon powders. For the different samples, all the X-ray diffraction patterns present broad peaks due to the presence of tetragonal $\mathrm{ZrO_2}$ with an average particles size about 15 nm, while amorphous carbon is not observed (Fig. 1). SEM images of the samples after pyrolysis reveal the presence of agglomerates about 2–3 μm, which are composed of $\mathrm{ZrO_2}$ nanoparticles and amorphous carbon (Fig. 2a). By means of backscattered SEM images (Fig. 2b), which do not show any contrast modulation inside an agglomerate, we confirm the good homogeneity of the ZrC precursor. The confirmation of carbon presence and its quantification was carried out by the mass variation occurring upon oxidative combustion under air. This mass loss was monitored by thermal gravimetric analysis TGA upon heat treatment of powders under air to 700 °C at 5 °C/min rate, followed by an isotherm (700 °C, 1 h). These results enable us to optimize the ZP/S molar ratio and Fig. 3 displays a typical TGA curve obtained for ZP/S = 3.2. The TGA curve is divided into two parts: a first mass loss up to approximately 150 °C, likely assigned to the loss of surface bond water and a second more important loss corresponding to the carbon oxidation, which is nearly completed at 480 °C. These

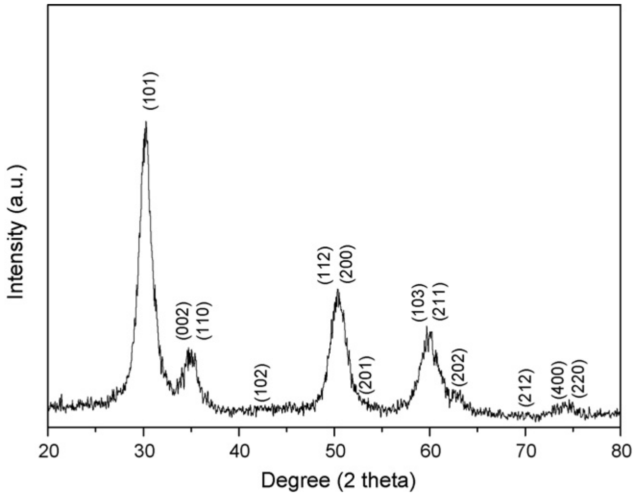

Fig. 1. X-ray diffraction pattern of the precursor obtained after heat treatment under flowing argon at 900 °C for 10 min.

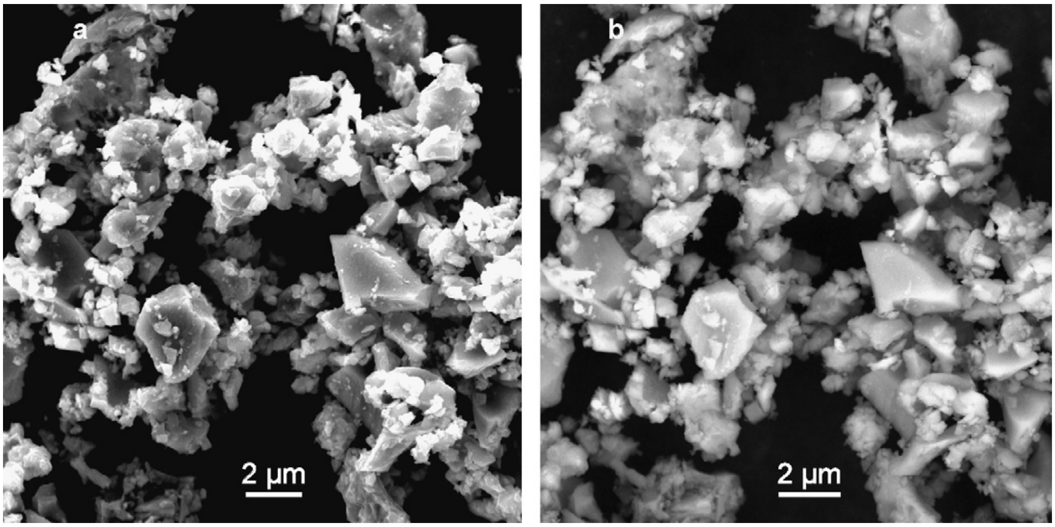

Fig. 2. (a) SEM image of the precursor obtained after heat treatment at 900 °C for 10 min and (b) corresponding SEM backscattered image.

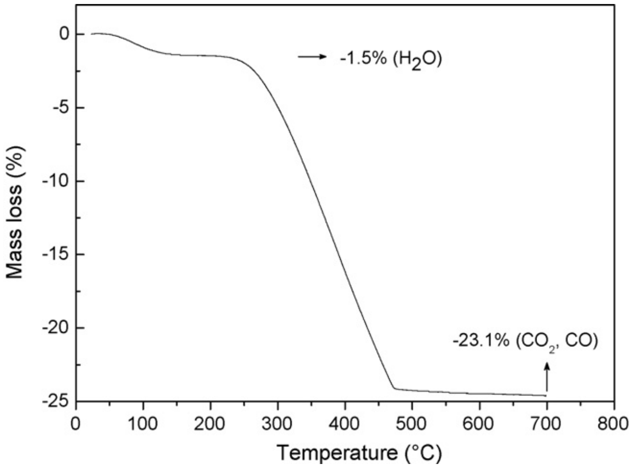

Fig. 3. TGA plot of mass loss vs. temperature for a 900 °C-pyrolyzed sample prepared with ZP/S = 3.2 (heating rate: 5 °C/min).

observations were confirmed by coupling the TGA analysis with a mass spectrometer to analyze the gas outlet. The carbon content for ZP/S = 3.2 is about 23.1 wt.%, which is equivalent to a C/Zr ratio of 3.12. The gel was then prepared by mixing 15 g saccharose and 0.14 mol of zirconium *n*-propoxide in 100 ml acetic acid. All the following results refer to this composition.

3.2. Heat treatments

Simultaneous TG/DSC experiments of the 900 °C pyrolyzed samples were performed in the temperature range 20–1400 °C at a heating rate of 10 °C/min under argon flow. Treatments were followed by a 3 h isotherm at 1400 °C in order to determine the time necessary to complete the carbothermal reduction. The curves (Fig. 4) show first a weight loss (3%) up to 400 °C corresponding to the evaporation of surface bond water, afterwards the mass remains constant up to about 1200 °C. An endothermic peak centered at 900 °C can be attributed to the reversed tetragonal to monoclinic phase transition of the zirconia. In fact, it is well known[21] that the tetragonal phase can be stabilized into nanosized grains thanks to their high surface energy. Since the mean grain-size increases on heating of the powder (by integration of contiguous grains), a reverse tetragonal to monoclinic transition can be observed for a critical grain-size. It can then be deduced from those results the grain-size of the zirconia particles is around 30 nm at the beginning of the carbothermal reduction. This is then the minimum grain-size to which the process can lead. These observations were confirmed by the X-ray diffraction patterns. Above 1200 °C, a mass loss coupled with a weak endothermal peak is observed corresponding to the onset of the carbothermal reduction, which seems to complete in 3 h at 1400 °C. The final mass loss associated to the reduction reaction is about 33.3%, whereas, for a stoichiometric mixture of zirconia and carbon, the mass loss for reaction (4) should be 35.17%. Since zirconia is not observed in XRD patterns of samples heat treated at 1400 °C, this indicates oxygen is still present in the samples and oxycarbides are then formed. Moreover, this also tells us free carbon is still present at the grain boundary.

In order to limit the crystallites size growth, a high heating rate was fixed (20 °C/min) to generate a competition between the size increase (evidenced by the zirconia phase transition) and the reduction reaction. By forming rapidly the refractory carbides at the interface between oxides particles, it may be expected the crystallites size growth will be slowed down. The diffraction pattern of the phase obtained at 1400 °C is reported on Fig. 5. Subsequent analysis by the Rietveld method enables to obtain a mean crystallites size of 93 nm for this sample and a cell parameter value $a = 4.690(1)$ Å. By increasing the temperature, the zirconium oxycarbide may further react with the free carbon still remaining in the sample to give a purer phase. However, our goal is to keep the particles size as small as possible and it is then important to find a good compromise between size and purity.

With this aim, two different samples were prepared by changing the heat treatment temperature (Table 1). Treatments at 1500 and 1600 °C were used to determine the temperature impact on the crystallites size and on the lattice parameter. A last experiment was carried out to determine the effect of a short heat

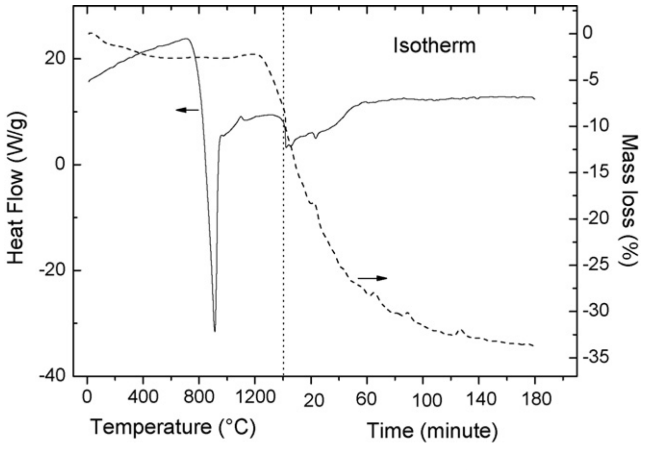

Fig. 4. Simultaneous TGA/DSC curves upon heating of the 900 °C-pyrolyzed sample under flowing argon (heating rate: 10 °C/min).

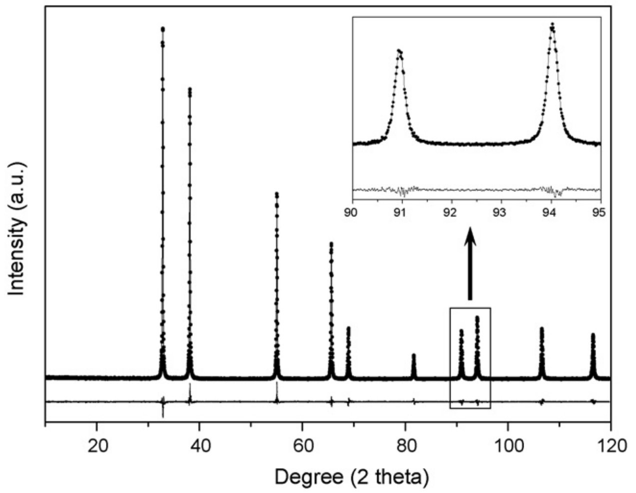

Fig. 5. Rietveld analysis of the X-ray pattern of the sample heat treated at 1400 °C for 3 h under argon flow (agreement factors: $R_{\mathrm{wp}} = 11.29\%$, $R_{\mathrm{B}} = 2.3\%$, Gof = 1.05).

Table 1
Summary of the different heat treatment sequences carried out under flowing argon

Sample	Isotherm (°C)	Dwelling time (min)
A	1400	180
B	1500	180
C	1600	180
D	1400, +1800	150, 6

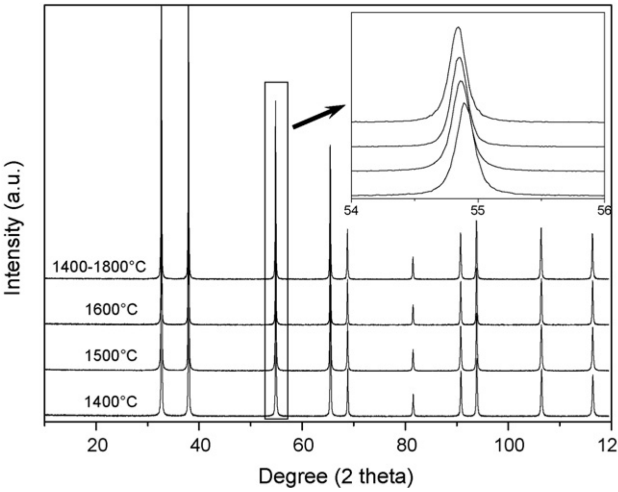

Fig. 6. Evolution of the XRD patterns of the different samples as a function of their respective heat treatment under argon flow.

Table 2
Evolution of the lattice parameter and of the mean crystallites size as a function of the applied heat treatment.

Temperature (°C)	Lattice parameter (Å)	Cristallites size (nm)
1400	4.690(1)	93
1500	4.694(6)	108
1600	4.695(9)	150
1400–1800 (6 min)	4.697(7)	110

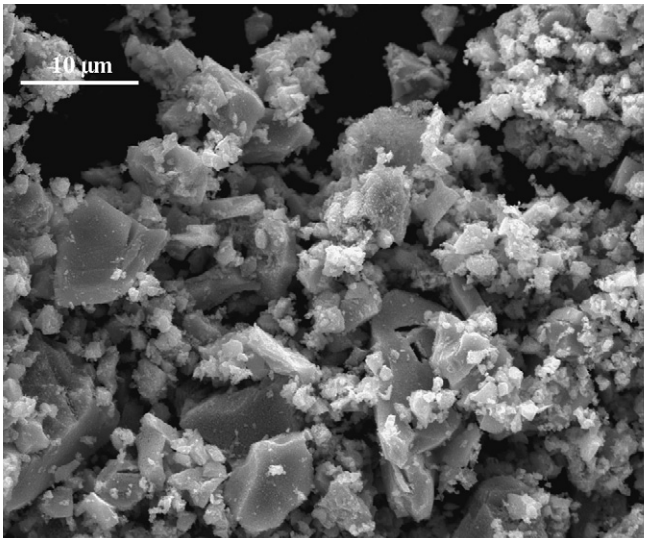

Fig. 7. SEM image of a sample heat treated at 1600 °C for 3 h (Sample C).

treatment above 1600 °C on a sample prepared at 1400 °C. The X-ray patterns and the refinement parameters for these samples are reported, respectively, in Fig. 6 and Table 2. XRD patterns indicate the formation of a single phase in all cases. Only a slight shift of the peaks to the low angles, dependent on the temperature, is observed. From these observations and as confirmed by Rietveld refinement, it is deduced that the lattice parameter increases when the temperature increases (Table 2).

In order to estimate the oxycarbides composition, we compared our lattice parameters with the ones from previous results.[22] After 3 h at 1400 °C, the composition is estimated to be $ZrC_{0.87}O_{0.08}$. Further temperature increases leads to $ZrC_{0.90}O_{0.05}$ at 1500 °C and to $ZrC_{0.92}O_{0.03}$ at 1600 °C. Even after heat-treatments at 1800 °C for 10 min, the composition corresponds to $ZrC_{0.93}O_{0.02}$. This clearly confirms the difficulty to obtain pure $ZrC_{0.98}$ (with reported cell parameter = 4.698 Å)[3,23] having nanosized grains by carbothermal reduction of a gel. Even if a higher temperature is favourable to the oxygen content decrease, it unfortunately has a negative counterpart on the particles size (Table 2) as the mean grain-size evolves from 93 nm at 1400 °C to 150 nm at 1600 °C. Heat treatments with several

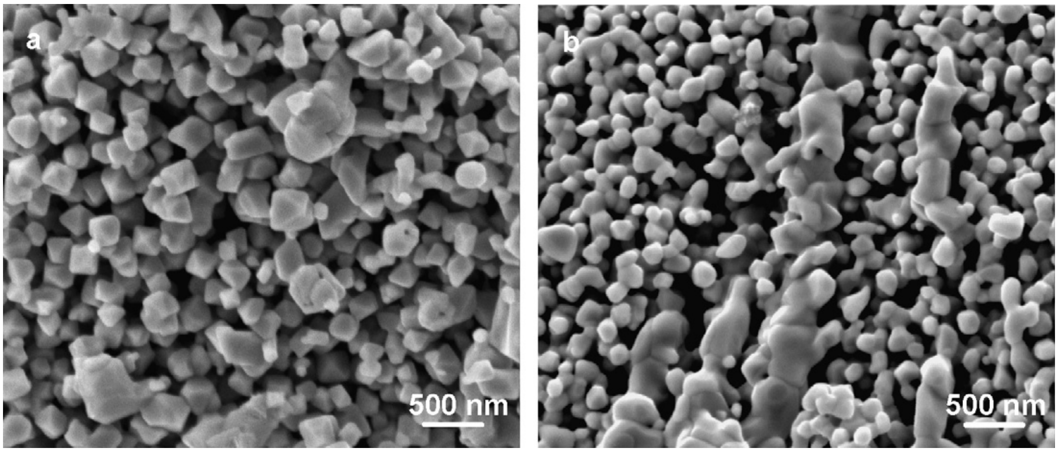

Fig. 8. (a) SEM image of an agglomerate microstructure for a sample heat treated at 1600 °C for 3 h (Sample C). (b) SEM image of an agglomerate microstructure for a sample heat treated at 1400 °C then at 1800 °C for 6 min (Sample D).

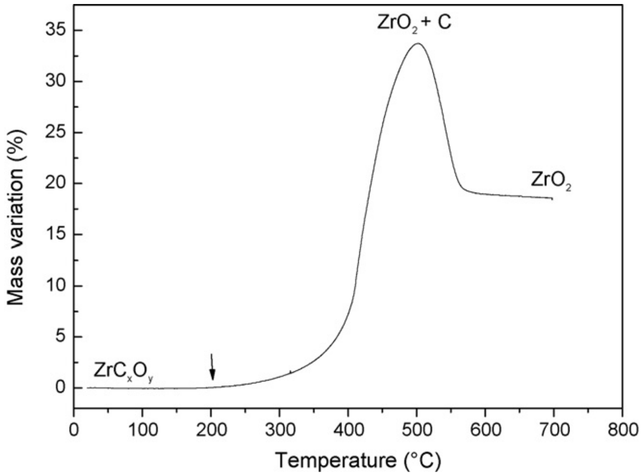

Fig. 9. TGA diagram of the oxidation of ZrC obtained after heat treatment at 1600 °C for 3 h (heating rate: 5 °C/min) (the arrow indicates the oxidation beginning).

temperature steps (Sample D) seem both to limit this growth and lead to purer phases as discussed above.

In order to confirm the sizes obtained from the XRD patterns, SEM observations of the powders obtained at 1600 and 1800 °C were also performed. Fig. 7 shows the presence of agglomerated individual grains with agglomerates size ranging from 1 to 10 μm, but observations at higher magnification clearly indicate the formation of nicely shaped octahedral particles at 1600 °C (Fig. 8a), which hardly started to sinter and to form small aggregates. Heat-treated samples at 1400 °C and at 1800 °C for 6 min (Fig. 8b) are different then, with particles smaller than after 3 h at 1600 °C. However, the particle's surface started to melt, resulting in particles looking more spherical and fused together. In both cases, the particles size distribution looks to be relatively homogeneous. In order to confirm these observations, thermogravimetric analyses upon carbides oxidation under air flow were carried out. Such experiments were reported by Roebuck et al.[24] to estimate the grain-size homogeneity of transition metal carbides. Our different samples were then oxidized and a typical TG curve is shown on Fig. 9. These studies illustrate the high reactivity of nanosized ZrC, which starts to oxidize under air at 200 °C, when the same measurements realized on microsized ZrC[22] show oxidation starts at about 300 °C. Another observation is that the ZrC oxidation takes place over a narrow temperature range, which indicates a relatively homogeneous grain-size distribution in the samples.

Depending on the desired applications, the presence of free carbon may not be a drawback. In such case, it is possible to get purer phases with smaller particles size by preparing precursors with higher C/Zr ratios. The carbothermal reduction performed at 1500 °C for precursors with C/Zr = 3.5 gives an oxycarbide with a lattice parameter of 4.696(4) Å and a mean particles size of 70 nm. If we compare these values with the ones obtained for C/Zr = 3.12, it is obvious the carbon excess plays a major role in limiting the particles growth and to decrease the residual oxygen content in ZrC. The carbon presence at the grain boundaries prevents the particles to be in contact and then it limits their growth; in the meantime, reactive carbon excess is still sufficient to maintain the carbothermal reduction leading to relatively high purity phases at lower temperature than in the case of lower C/Zr ratios. Nevertheless, such reactions end up with significant free carbon content at the grain boundaries, which is not suitable in the preparation of preceramic materials. In fact, this carbon remains at the grain boundaries and it will be responsible for the poor powders densification during the sintering step and low mechanical properties of the dense product.

4. Conclusion

A new simple sol–gel route was developed using zirconium *n*-propoxide, saccharose as carbon source and acetic acid as chemical modifier of the zirconium alkoxide. Pyrolysis of the obtained polymeric gels under flowing argon transforms them into precursors consisting of intimately mixed nanosized tetragonal zirconia and reactive amorphous carbon. Further heat treatments of these precursors end up with the carbothermal reduction of the oxide particles and the formation of nanosized oxycarbides. The obtained powders after different heat treatments sequences were investigated using XRD, thermal analysis and SEM. It was proved the oxygen content can be decreased by increasing the heat treatment temperature (from 8 at.% at 1400 °C to 3 at.% at 1600 °C); however, it is detrimental to the grains size ranging from 90 nm at 1400 °C to 150 nm at 1600 °C. In order to obtain powders as pure as possible with small grains size, it was necessary to perform heat-treatments with several temperature steps or to prepare precursors with a higher C/Zr ratio (>3).

Acknowledgments

Experimental contributions by B. Beaudoin (SEM observations – LRCS/CNRS, Amiens) and by G. Boemare (TGA/DSC experiments – SPMS-ECP/CNRS, Chatenay-Malabry) are acknowledged. This work was supported by the CEA/CNRS research program ISMIR.

References

1. Bouchard, J., IAEA International conference on 50 years of nuclear power—the next 50 years. *Book Extended Synopses*, 2004, **234**, 22–23.
2. Billot, P., Conference on basic studies in the field of high-temperature engineering, Paris (France) OECD-NEA, 2004, *Vol. 277*, pp. 41–66.
3. Gusev, A. I., Rempel, A. A., Magerl, A. J., Disorder and order in strongly non-stoichiometric compounds, transition metal carbides, nitrides and oxides, Materials Science, 2001, *Vol. 47*, Springer-Verlag.
4. Storms, E. K. and Wagner, P., Thermal conductivity of sub-stoichiometric ZrC and NbC. *High Temp. Sci.*, 1973, **5**, 454–462.
5. Andrievskii, R. A., Vlasov, K. P., Shevshenko, A. S., Lanin, A. G., Pritchin, S. A., Klyushin, V. V., Krushin, S. P. and Maskaev, A. S., Influence of reactor irradiation on the physico-mechanical properties of zirconium and hafnium carbides. *Inorg. Mater.*, 1977, **14–4**, 530–533.
6. Minato, K., Ogawa, T., Sawa, K., Ishikawa, A., Tomita, T., Iida, S. and Sekino, H., Irradiation experiment on ZrC-coated fuel particles for high temperature gas-cooled reactors. *Nucl. Technol.*, 2000, **130**, 272–281.
7. Darolia, R. and Archbold, T. F., Plastic deformation of polycrystalline zirconium carbide. *J. Mater. Sci.*, 1976, **11**, 283–290.

8. Siegel, R. W., "Mechanical Properties of Nanophase Materials", In Synthesis and Properties of Mechanically Alloyed and Nanocrystalline Materials, In Fiorani, D., Magini, M., eds., Mater. Sci. Forum, 1997, 235–238, pp. 851–860.
9. Lu, Y. and Liaw, P. K., The mechanical properties of nanostructured materials. *JOM*, 2001, **53–3**, 31–35.
10. Amato, I., Mechanical properties of nanostructured ceramic materials. *Mater. Sci. Forum*, 2004, **455–456**, 550–555.
11. Wan, J., Duan, R.-G., Gasch, M. J. and Mukherjee, A. K., Highly creep resistant silicon nitride/silicon carbide nano–nano composites. *J. Am. Ceram. Soc.*, 2006, **89**, 274–278.
12. Preiss, H., Schultze, D. and Klobes, P., Formation of NbC and TaC from gel-derived precursors. *J. Eur. Ceram. Soc.*, 1997, **17**, 1423–1435.
13. Preiss, H., Berger, L.-M. and Schultze, D., Studies on the carbothermal preparation of titanium carbide from different gel precusors. *J. Eur. Ceram. Soc.*, 1999, **19**, 195–206.
14. Sacks, M., Wang, C.-A., Yang, Z. and Jain, A., Carbothermal reduction synthesis of nanocrystalline zirconium carbide and hafnium carbide powders using solution-derived precursors. *J. Mater. Sci.*, 2004, **39**, 6057–6066.
15. Sanchez, C., Livage, J., Henry, M. and Babonneau, F., Chemical modification of alkoxide precursors. *J. Non-Cryst. Solids*, 1988, **100**, 65–76.
16. Preiss, H., Berger, L.-M. and Szulzewsky, Thermal treatment of binary carbonaceous/zirconia gels and formation of Zr(C,O,N) solid solutions. *Carbon*, 1996, **34**, 109–119.
17. Yi, G. and Sayer, M., An acetic acid/water based sol–gel PZT process I: modification of Zr and Ti alkoxides with acetic acid. *J. Sol–Gel Sci. Technol.*, 1996, **6**, 65–74.
18. Bérar, J.-F. and Baldinozzi, G., Xnd Code: From X-ray Laboratory Data to Incommensurately Modulated Phases. *Rietveld Modelling of Complex Materials, IUCR-CPD Newsletter*, *20*., 1998.
19. Doeuff, S., Henry, M., Sanchez, C. and Livage, J., Hydrolysis of titanium alkoxides: Modification of the molecular precursors by acetic acid. *J. Non-Cryst. Solids*, 1987, **89**, 206–216.
20. Livage, J., Henry, M. and Sanchez, C., Sol–gel chemistry of transition metal oxides. *Prog. Solid State Chem.*, 1988, **18**, 259–341.
21. Baldinozzi, G., Simeone, D., Gosset, D. and Dutheil, M., Neutron diffraction study of the size-induced tetragonal to monoclinic phase transition in zirconia nanocrystals. *Phys. Rev. Lett.*, 2003, **90**, 216103.
22. Maitre, A. and Lefort, P., Solid state reaction of zirconia with carbon. *Solid State Ionics*, 1997, **104**, 109–122.
23. Storms, E. K., The refractory carbides. *Refractory Materials*, *Vol. 2*. Academic, New York, 1967.
24. Roebuck, B., Almond, E. A. and Kellie, J. L. F., Characterization of the particle size of cubic transition metal carbides by measurements of the rate of oxitdation, Horiz. Powder Metall., Proc. Int. Powder Metall. Conf. Exhib., *Vol 1*. In Kaysser W., Huppmann W., Schmid W., Freiburg, eds., 1986, pp. 123–126.